Complex Synchronization Phenomena in Ecological Systems

Lewi Stone*, Ronen Olinky*, Bernd Blasius†, Amit Huppert* and Bernard Cazelles**

*Biomathematical Unit, Life Sciences, Tel Aviv University, Ramat Aviv, 69978, Israel
†Institute of Physics, University of Potsdam, Am Neuen Palais 10, D-14469 Potsdam, Germany
**CNRS UMR 7625 - Universite Pierre et Marie Curie, 7 quai Saint Bernard, case 737, 75252 Paris, France.

Abstract.
Ecological and biological systems provide us with many striking examples of synchronization phenomena. Here we discuss a number of intriguing cases and attempt to explain them taking advantage of a modelling framework. One main focus will concern synchronized ecological end epidemiological cycles which have Uniform Phase growth associated with their regular recurrence, and Chaotic Amplitudes – a feature we term UPCA. Examples come from different areas and include decadal cycles of small mammals, recurrent viral epidemics such as childhood infections (eg., measles), and seasonally driven phytoplankton blooms observed in lakes and the oceans. A more detailed theoretical analysis of seasonally synchronized chaotic population cycles is presented.

INTRODUCTION

Synchronization is a phenomenon that is as important as it is widespread in ecological systems. Consider Australia's Great Barrier Reef. Here many coral species have the remarkable ability to tune their reproductive cycle with astonishing precision. On a single day each year, just after the November full moon, corals synchronize by collectively releasing millions of gametes in a remarkable large-scale mass-spawning event, whose purpose is to enhance the survival of the next generation. Similar large-scale synchronization phenomena may be found in the insect world. Certain Asian firefly species are famous for their ability to gather in dense swarms where they rhythmically flash on and off in perfect unison, in a synchronized display of courtship. Equally curious is the manner in which many animal populations oscillate in a chaotic fashion but are nevertheless able to collectively synchronize over enormous spatial scales, sometimes over continents. For the classic ten-year Canadian hare-lynx cycle, populations from different regions have been tightly synchronized for hundreds of years now, creating one of Ecology's greatest enigmas. Major human epidemics are also synchronized both spatially and temporally, as the disease spreads in waves through a network of interconnected suburbs. Here we review various aspects of ecological synchronization and methods that have been adopted to model the many aspects of this phenomenon.

CP622, *Experimental Chaos: 6th Experimental Chaos Conference*, edited by S. Boccaletti et al.

THE EVOLUTION OF SYNCHRONIZATION STRATEGIES

A perplexing question that did not escape the notice of some of the greatest thinkers working in evolutionary theory can be stated very simply: "Why do synchronized behavioral strategies evolve over evolutionary time?" Unfortunately there is no straightforward answer to this innocent looking question. Many bird species, for example, prefer to breed together in a synchronized mating season at much the same time each year (for reasons not necessarily connected to climatic conditions), while other related species breed continuously throughout the year and show no such signs of synchronized behavior. Why does one species synchronize and not the other? Many similar questions are still a great puzzle for biologists. Nevertheless, evolutionary arguments have made some important successes, and we briefly summarize an interesting model attributed to Maynard Smith [1].

In the last few decades, reproductive synchrony has often been considered a sexual strategy adopted by the female sex and forced on the entire population to decrease the likelihood of the male deserting his partner. Should a male attempt to cheat, he will probably find the mating season too short to allow him time to find and mate with a new partner. He will inevitably lose by running from, rather than investing in, his offspring. Thus it is to the females advantage to keep the mating season synchronized and short. In other words, synchronization has evolved to prevent males cheating on their partners. Maynard Smith's evolutionary model is simple and elegant, and begins by assuming that if both parents are involved in raising their young, the number of surviving offspring is v_2. However, if the male deserts on his partner, only v_1 young will survive (with $v_1 < v_2$). Now suppose that there is a probability p that a male will desert his partner after she has laid eggs, and then succeeds to mate with another female. The fitness of such a deserting male is determined by the number of offspring he produces, which is on the average $v_1 + pv_2$. Thus desertion will be favored (or is an evolutionary stable strategy) only if $v_1 + pv_2 > v_2$ i.e., if

$$p > \frac{v_2 - v_1}{v_2}. \tag{1}$$

Hence desertion is favored only if there is a good chance (p) of the male finding and mating with a second partner. Note that should the female force a short synchronized breeding season on the male, this acts to reduce p, and increase her chances that the male will stay and help raise their young. So it is a worthwhile strategy for females to synchronize their breeding season. In recent years behavioural ecologists have far more sophisticated arguments for understanding parental care and reproductive synchrony - our aim here was to provide a glimpse into the sometimes unusual approaches used in evolutionary models.

There are many other types of synchronized reproductive strategies, and they are often context dependent. As we have mentioned, some corals, spawn on a single day every year. It is believed that this is either to 'fool' predators or to minimize their impact through 'predator satiation.' Similarly, different coral species spawn in different months (i.e., with phase lags between events) possibly to prevent hybridization of different species and/or as a mechanism to release larvae from interspecific competition. Cicadas in America periodically emerge with regular synchronized cycles of prime number

intervals of 7 or 13 years. Evolutionary theorists try to explain the vexing question: "Why prime?"

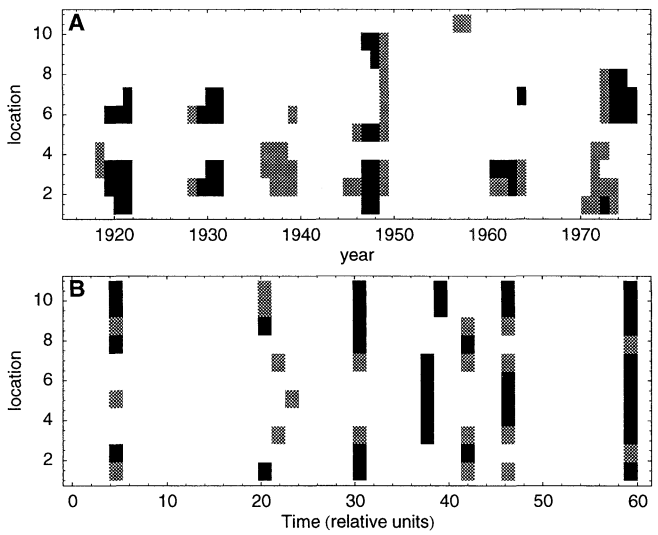

FIGURE 1. a) Occurence of outbreaks of Lepidoptera (Douglas-fir tussok moth) in British Columbia (Canada) from 1916 - 1976, at 11 locations. Data from [2]. b) Simulation of a CML of 11 subpopulations modelled by the Ricker model. The synchronized state ($x_i = x_j$ for all i, j) is unstable but one can observe imperfect synchrony. Black color: severe outbreak ($x > 0.70 \max(x_i)$); grey color: moderate outbreak ($x > 0.40 \max(x_i)$); white color: no outbreak.

SYNCHRONIZED POPULATION OSCILLATIONS AND EXTINCTIONS

Physicists often study the dynamics and synchronization of Coupled Map Lattices (CML's, see eg., [3]). But this also proves to be highly relevant for studying ecological systems [4]. Fig.1a shows the occurence of outbreaks of Lepidoptera (tussock moths) at 11 locations spread over 100's of kilometers across Canada (from [2]). Note the erratic synchronized patterns which probably originate from factors other than environmental cues. The dataset raises several problems which CML models may help in exploring. For example: Why are there apparent population cycles? Why are the populations synchronized? And why is the synchronization erratic?

To gain insight into this 'imperfect' synchronization, imagine a spatial landscape of interconnected patches, each with its own subpopulation subject to the usual localized birth-death growth process (eg., the simple logistic equation is a useful model here). The following CML model may then be set up:

$$x_i(t+1) = \sum_{j=1}^{N} m_{ij} F(x_j(t)). \tag{2}$$

Here $x_i(t)$ represents the population of the i'th patch, and m_{ij} describes the migration from patch-j to patch-i. The term $F(x_j)$ models the birth death process of the populations, and might typically be the logistic model $F(x) = rx(1-x)$ or the Ricker model $F(x) = x \cdot e^{r(1-x)}$.

The criterion for the fully synchronized state ($x_i = x_j$) for all i, j is well known (eg., [3, 5]) and depends on the subdominant eigenvalue λ of the dispersal matrix M, and the Lyapunov exponent μ of a single (uncoupled) one-dimensional map F. Full (or 'perfect') synchronization is assured if the transverse Lyapunov exponent ($\mu_\perp$) of system 2 satisfies:

$$\mu_\perp = \mu + \ln(|\lambda|) < 0. \tag{3}$$

For parameters that violate this criterion it is possible to arrive at states of 'imperfect synchrony.' However the above criterion is based on long-term average quantities (eg., $(\mu, \mu_\perp)$). In the case of complex dynamics (chaotic or stochastic) these quantities may fluctuate and their distributions may explain unexpected dynamics (eg., riddled basins, on-off intermittency). Hence even when the invariant synchronous manifold is stable $\mu_\perp \approx< 0$, there can still be initial conditions for which the transverse instantaneous Lyapunov exponent becomes weakly positive and trajectories can jump to another attractor. This effect can produce dynamics with riddled basins: depending on initial conditions one can observe both perfect and imperfect synchrony. Conversely, when the synchronous manifold is weakly unstable ($\mu_\perp >\approx 0$), it is still possible to observe synchronized dynamics although this behaviour may be interrupted by on-off intermittency [6].

Fig.1b displays simulations of a metapopulation of $N = 11$ subpopulations (CML) connected via nearest neighbour coupling with the Ricker model taken for F. Parameters values used are $r = 6.5$ and the dispersal coefficient is $m = 0.35$. In this particular case, the synchronized state ($x_i = x_j$ for all i, j) is unstable but one can observe 'imperfect synchrony' due to the development of synchronized chaotic population clusters. Very similar erratic synchronization can emerge for other reasons. For example, with globally coupled populations, when $r = 4$, $m = 0.35$ the synchronized state ($x_i = x_j$ for all i, j) is weakly unstable and the On-Off intermittency produces synchronized patterns very similar to the observed data.

Spatial synchronization is a phenomenon that was studied by ecologists in the late 1970's well before CML's became popular in the physics literature. Den Boer, for example, from the Netherlands realized from his field work that migration between patches tends to enhance synchronization of the larger metapopulation. As such, synchronization could create conditions that were sometimes uniformly bad for all local populations. Synchronized patch populations that periodically attained dangerously low levels, could more easily become globally extinct. On the other hand, asynchrony between patches acts to prevent global extinction. At any point in time some local populations increase and act as source populations that (through migration) prevent the disappearance of declining sink populations. The conditions for synchrony, asynchrony and chaotic dynam-

ics in CML's are thus of interest for ecologists who use these models in an attempt to understand the dynamics of population extinctions and its relation to asynchrony.

PHASE SYNCHRONIZATION OF CHAOTIC POPULATION CYCLES

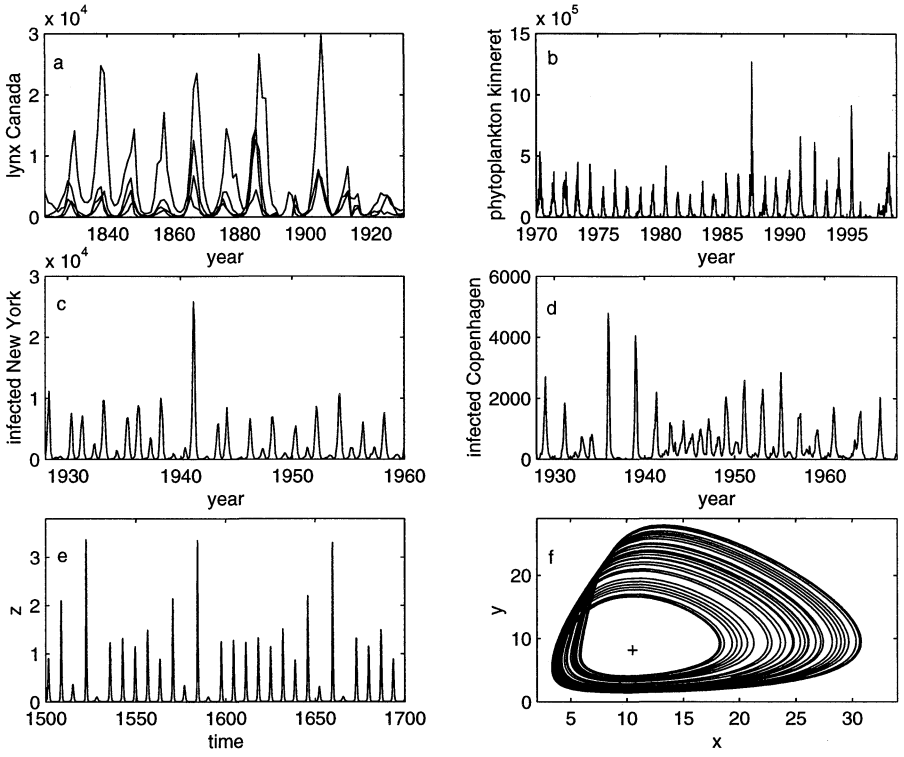

FIGURE 2. a) 10 year cycle in the Candian lynx record 1820-1930, plotted for seven separated districts in Canada; b) phytoplankton bloom in Lake Kinneret, Israel (with kind permission of Prof. Utza Pollingher); c) Number of cases of measles in New York City 1920-1960 and d) Copenhagen 1920-1970; e) simulated UPCA dynamics from (4) and f) $x-y$ phase plane with parameters: $a=b=1, c=10, k=0.1, e=0.6, x_0=1.5, y_0=0, z_0=0.01$.

We are also studying synchronized population oscillations, such as those observed in Canada's unusual 10-year hare-lynx cycle (Fig.2a). These populations have the intriguing feature of highly erratic or chaotic abundances but remarkably constant period length – a behaviour we refer to as UPCA (Uniform Phase evolution with Chaotic Amplitudes). As yet, conventional ecological models have failed to reproduce this behaviour, despite the fact that UPCA is an important and commonly observed ecological and biological dynamic. It has been noted in many systems, ranging from small mammal populations

to neural network oscillations. Recently, we designed a simple deterministic foodweb model that generates chaotic UPCA oscillations [7, 8] (Fig.2e,f & Legend):

$$\begin{aligned} \dot{x} &= a(x-x_0)-kxy \\ \dot{y} &= -b(y-y_0)+kxy-eyz \\ \dot{z} &= -c(z-z_0)+eyz. \end{aligned} \tag{4}$$

The UPCA dynamics of this model may be explained in simple terms as follows. Firstly, note that the model has three unstable equilibrium points. The relevant equilibrium in the positive orthant may be approximated for $y_0, z_0 \ll 1$ as

$$x^* = b/k, \quad y^* = a/k - ax_0/b, \quad z^* = cz_0/(c-ey^*). \tag{5}$$

For the given parameters, $(x^*, y^*, z^*) \approx (10, 8.5, 0.1)$ and this forms the centre of an unstable oscillation which spirals with increasing radius about the point (x^*, y^*) in the $x-y$ plane ($z \approx 0.1$, see Fig.2f). When y increases beyond the critical threshold level, $\tilde{y} = c/e$, the z-variable 'triggers' and the trajectory shoots rapidly out of the plane $z \approx 0$ only to be reinjected back, soon after, to return close to the fixed point (x^*, y^*, z^*). These dynamical features have similarities to the Rössler equations, the main difference being that now all populations are always positive - a realistic feature that is nontrivial to implement [8].

Linearizing the equations about the equilibrium and taking eigenvalues of the resulting Jacobian makes it possible to approximate the frequency of the system as

$$\Omega = \sqrt{ab - akx_0 - (akx_0/2b)^2}. \tag{6}$$

Ω quantifies the 'frequency' of the trajectory as it spirals about the unstable equilibrium in the $x-y$ plane, and the estimate is of good accuracy according to numerical simulations. The result is useful for synchronization studies where fine control of oscillator frequency is often required. Note that for $x_0 = 0$, the result simplifies to $\Omega = \sqrt{ab}$ as it should for the classical Lotka-Volterra equation.

Examining more closely the Canadian hare-lynx cycle (Fig.2a), one notes that although the lynx populations of many different regions phase-lock to the same extraordinary collective rhythm, their peak population abundances are nevertheless chaotic and largely uncorrelated to one another. What makes this so peculiar is that there is synchronization in phase or rhythm, but not in amplitude; in other words, this is a clear case of 'phase-synchronization.' The ecological UPCA model provides us with a tangible system for exploring this form of complex chaotic synchronization and, in fact, phase-synchronization immediately emerges upon coupling several UPCA foodweb models of different frequencies Ω_i via diffusive migration. We have investigated spatially extended systems by examining a spatial lattice of patches, where each patch is a single UPCA foodweb model. Such a 'metacommunity' could, for example, represent the Canadian hare-lynx system when viewed over a large spatial scale. Nonidentical model foodwebs with random natural frequencies that act as spatial 'inhomogeneities' over the lattice induce interesting dynamics. In the regime of phase-synchronization, synchronized patch

populations are typically separated by a phase lag which can give rise to complex spatio-temporal patterns [7, 8]. Often a remarkable chaotic travelling wave structures are produced, where population abundances remain chaotic, but unusual circular waves form and spread in time across the spatial landscape. Ecological field studies of synchronized populations (eg plant, plankton, vole, hare-lynx populations) have reported similar travelling wave structures.

SEASONALLY DRIVEN UPCA POPULATION DYNAMICS

Another important aspect of synchronization is the manner in which ecological communities entrain to periodic environmental or climatic driving variables [9, 10]. In Lake Kinneret (Sea of Gallilee), Israel, for example, seasonal stratification and nutrient availability patterns ensure that almost every March a large-scale algae bloom appears (see Fig.2b). As in many other freshwater lakes, the presence of a phytoplankton bloom signals dangerous nutrient loading (eutrophication) and water quality problems. The seasonal forcing adds a complicating factor to the study of bloom dynamics since it can induce irregular chaotic oscillations synchronized to the seasonal cycle. This is a form of synchronization through unidirectional coupling or one-way driving. Including seasonal forcing such a model in dimensionless variables would read as [11]:

$$\begin{aligned} \dot{N} &= I - \beta(t)NP - qN \\ \dot{P} &= \beta(t)NP - P, \end{aligned} \tag{7}$$

where N represents nutrients and P represents phytoplankton in the water column. The two dimensionless parameters I and q are an effective influx and nutrient loss rate respectively. The seasonal forcing is given by the yearly periodic function $\beta(t)$ and could be represented by

$$\beta(t) = 1 - \alpha\cos(\omega t). \tag{8}$$

Seasonal forcing induces UPCA dynamics that are generally phase locked to the seasonal cycle. Although we have succeeded in obtaining the desired goal of generating UPCA dynamics from a periodically forced model, Eqns. (6,7) lead to behaviour that is to some degree unrealistic for describing phytoplankton dynamics. In our simulations it is often the case that many years go by without algae blooms occurring. These 'skippings,' which we discuss further below, are not desirable but appear to be intrinsic to the forced model (7). Nevertheless, with subtle modifications [11], we have succeeded in constructing a seasonally forced model that generates the desired UPCA behaviour producing simulations similar to Fig.2e,f.

EPIDEMIOLOGY

In the same spirit but in the context of epidemiology synchronization has great control over the (often chaotic or irregular) dynamics of diseases as they spread through complex networks of suburbs and cities. Here we concentrate on the dynamics of childhood

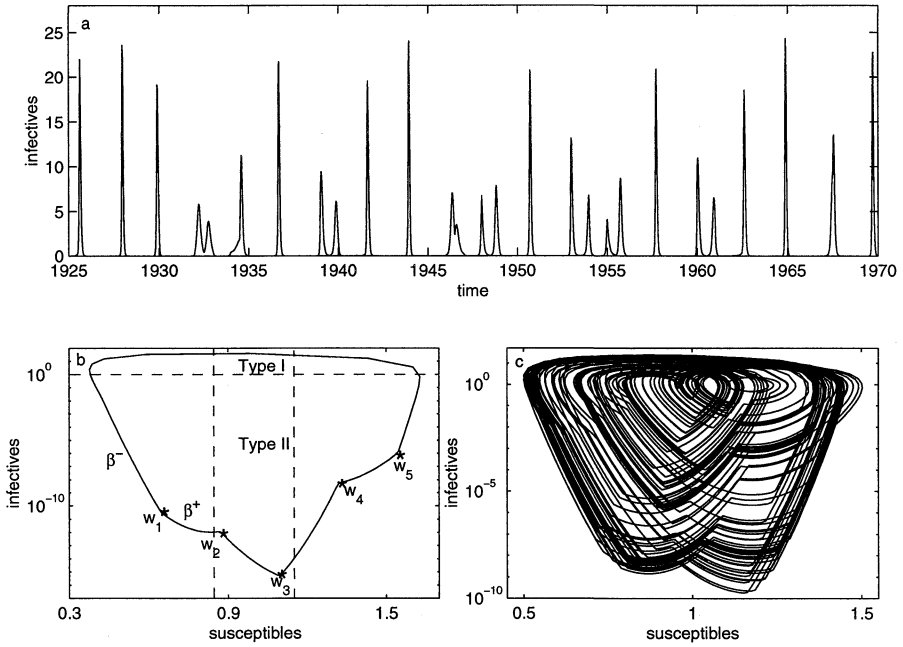

FIGURE 3. Simulation results of the epidemic model (9) in the UPCA region. a) Chaotic time series exhibiting years of fade-outs or 'skips' when the epidemics fail to trigger. b) Illustratory phase plane diagram with logarithmic scale for infectives. Type I solutions (major epidemics) occur in upper portion of phase plane above the i-nullcline (dashed horizontal line). Type II solutions appear below i-nullcline. The vertical dashed lines represent the s-nullclines for the two different seasons. The w_i demark the points in the phaseplane when the seasons change and the s-nullcline jumps from β^- to β^+ or vice-versa. c) The phase plane diagram of the time series in (a).

diseases such as measles which are also entrained by an annual seasonal cycle - the epidemics usually coincide with the beginning of the school year. The oscillations are irregular (see measles in New York City and Copenhagen displayed in Figs.2c,d) being characterized by inherent UPCA-like dynamics. Yet conventional epidemiological models are incapable of reproducing this behavior. The UPCA models we are developing provide a technical-fix and form the basis of a theoretical study of the spread of epidemics.

Our focus here is on the synchronization of measles to the seasonal cycle and address the interesting problem of 'fade-out' dynamics. Namely, in some years the epidemic fails to take off at some locations (as in Copenhagen), while at other locations fade-outs are less frequently or never occur (as in New York).

We start with the standard SIR model for epidemics

$$\begin{aligned} \dot{S} &= \mu - \mu S - \beta_0 \beta(t) SI \\ \dot{I} &= \beta_0 \beta(t) SI - \gamma I \\ \dot{R} &= \gamma I - \mu R. \end{aligned} \tag{9}$$

Here, S, I, R represent the density of susceptible, infected and recovered individuals, respectively, in a constant population of size $N = S+I+R = 1$, scaled to unity without loss of generality. The average life span of an individual and the infectious period are given by μ^{-1} and γ^{-1}, respectively. The infection contact rate is given by $\beta_0\beta(t)$ which is a periodic function of time that takes into account seasonality. Here, we use a square wave forcing with amplitude δ, so that

$$\beta(t) = (1 \pm \delta). \tag{10}$$

The year is divided into two seasons, each of time T. In winter $\beta(t) = \beta^+ = (1+\delta)$ while in summer $\beta(t) = \beta^- = (1-\delta)$. Typical parameter values for measles are $\mu = 0.02$, $\gamma = 75$. For the infection rate we set $\beta_0 = 1700$ and δ varies from $\delta = 0.15$ to $\delta = 0.2$ [5].

After a change of variables, the equations read

$$\begin{aligned} \dot{s} &= m(1-\beta(t)si) - \mu s \\ \dot{i} &= \gamma i(\beta(t)s - 1). \end{aligned} \tag{11}$$

where we have introduced

$$i = \frac{\gamma}{\mu} I, \quad s = \frac{\beta_0}{\gamma} S, \quad m = \frac{\mu\beta_0}{\gamma}. \tag{12}$$

Note the structural similarity between the epidemic model eqns. (10) and the phytoplankton model (6), hinting that the dynamics of epidemics and phytoplankton blooms might not be unrelated. Fig.3a provides a time-series of the SIR equations in which the dynamics are chaotic. Since the numbers of infected can change many orders of magnitudes during an epidemic outbreak it is useful to describe the infected numbers by their logarithm, $w = \log i$. Fig.3c shows the solution in (s,w) phase space. Note, that epidemics are strongly phase locked and occur at roughly the same time every year. For some years, however, epidemics do not appear to trigger at all. These are the above mentioned 'skips' or fadeouts that are characteristic of the observed data.

Analytical solutions

In the following analysis we will reconstruct the phase plane by explicit expressions in order to understand the dynamical foundations of epidemic fadeouts. In the process we sketch a method for constructing a first return map that approximates the dynamics of system (9). We make use of the fact that the number of infected individuals change many orders of magnitude during a typical epidemic (see also Schartz et al. [12] who use a similar approach to describe a forced laser systems). Note, that the scaled variable s in (1) is of the order of 1, so that the susceptible death term $-\mu s$ in the first equation of (11) can be neglected with no major effect on the dynamics in the parameter regime of interest.

When $i \gg 1$ we approximate (11) as

$$\begin{aligned} \dot{s} &= -m\beta(t)si \\ \dot{i} &= \gamma i(\beta(t)s - 1), \end{aligned} \tag{13}$$

and when $i \ll 1$ (11) may be approximated as

$$\begin{aligned} \dot{s} &= m \\ \dot{i} &= \gamma i(\beta(t)s - 1). \end{aligned} \tag{14}$$

These approximations distinguish two solution types in the phase plane. A solution of the first system would be referred as Type I solution. This solution approximates trajectories located above the s nullcline which lies on the horizontal $i = \frac{1}{\beta s} \approx 1$. Type II solutions approximate trajectories below this nullcline and are solutions of (14).

In Type I solutions, during an epidemic the infected population i changes by many orders of magnitude, while the susceptible population s is always decreasing. Type II solutions are characterized by small numbers of infected individuals, while the susceptibles s are always increasing. The rate of change of s is characterised by different time scales and is slow for Type II solutions but very fast for Type I. Therefore, the system spends most of its time in solution Type II, characterised by minimal infected numbers and a slow build up of susceptibles.

In the following analysis we will make use of the property that the i -nullcline is a straight line located at $s = 1/\beta^{\pm}$. These nullclines are marked as vertical dotted lines in Fig.3b. The effect of seasonality can be regarded as a periodical jump in the horizontal position of this nullcline from $s = 1/\beta^{-}$ to $s = 1/\beta^{+}$ (or vice-versa).

Type I

Eqns. (13) is the well known SIR epidemic model with solution

$$\frac{m}{\gamma}(i(t) - i_0) = s_0 - s(t) + \frac{1}{\beta^{+}} \ln \frac{s(t)}{s_0}. \tag{15}$$

Note that Type I solutions are initiated when the trajectory crosses the s-nullcline and enters the upper half of the phase plane (Fig.3b). This entry point is the end point of solutions of Type II which we specify shortly. For now asume that the forcing function β^{+} remained constant over the entire epidemic period. In this scenario the maximum number of individuals i_m is reached when $s(t) = \frac{1}{\beta^{+}}$, which gives

$$i_m = \frac{m}{\gamma}(s_0 - \frac{1}{\beta^{+}} + \frac{1}{\beta^{+}} \ln \frac{1}{(\beta^{+})s_0}) + i_0. \tag{16}$$

In the scenario where the forcing jumps during the epidemic build up it is possible to derive a suitable formulation for i_m.

The epidemic ends when the infective population crosses the s-nullcline (approximately when $i = 1$ or $w = \log i = 0$). At this point the trajectory passes to Type II solutions with initial conditions that can now be determined easily from (15).

Type II

Recall that a year is taken to have only two seasons. It starts in summer at times $t_n, \quad n = 0,2,4,..$ and a low infection rate $\beta^- = 1-\delta$, followed by winter at times $t_n, \quad n = 1,3,5,..$ with high infection rate $\beta^+ = 1+\delta$. Each season is half a year long ($T = \frac{1}{2}$). The overall strategy for solving the system (14) is to calculate the solution in the time intervals between t_n and t_{n+1}. Each time interval will have a constant infection rate (i.e. either β^+ or β^-) and inital values s_n and w_n. For the case of Type II solutions we assume that at time t_0, $\beta(t) = \beta^-$ and the inital conditions are s_0 and $w_0 = 0$.

First, observe that the susceptibles are always increasing with constant rate $s(t) = mt + c_0$ where $c_0 = s_0 - mt_0$. From the phase plane (Fig.3b) we see that the point (s_1, w_1) is a sharp point that results from the change of $\beta(t)$ as it jumps from β^- to β^+. All sharp points (s_n, w_n) are produced by this mechanism. By integrating system (14) between two neighboring sharp points we get

$$\frac{w_1 - w_0}{\gamma} = \frac{w_1}{\gamma} = \beta^- \int_{t_o}^{T} s(t)dt - T + t_0 = \beta^- \int_{t_o}^{T} mt + c_0 dt - T + t_0 \tag{17}$$

$$\frac{w_{n+1} - w_n}{\gamma} = \beta^{\pm} \int_{nT}^{(n+1)T} s(t)dt - T \tag{18}$$

which enable us to express w_n in recursive form to ultimately obtain:

$$\frac{w_n}{\gamma} = \frac{1}{8}m[n^2 + (-1)^n n\delta] + \frac{1}{2}[n(c_0 - 1) + \frac{\delta}{2}c_0((-1)^n - 1)] - c_1 \tag{19}$$

where $c_1 = \frac{1}{2}t_0^2(1-\delta) + t_0((1-\delta)c_0 - 1)$ and $T = 1/2$ This recursive scheme stops whenever $w_n > 0$. At this point we return back to Type I solutions.

A point where the infected population function reaches a local maximum w_m and $w_m < 0$ is referred as a skipping point. This is because in the case $w_m > 0$ an epidemic could have otherwise been triggered. The difference between a skipping point and an epidemic peak is not just a question of magnitude. During a skipping point the susceptible population continues to build up, while at an epidemic peak the susceptible population declines. From the real data we know that different cities manifest different skipping dynamics. By this analysis of the Type II solution we can deduce the maximum number of skips from the system parameters. Let us define N to be the smallest n where $w_n > 0$, then the overall number of skips is given by $N/2$.

We have extended the argument to show that the number of skips

$$N \sim \frac{1}{m} = \frac{\gamma}{\mu\beta_0}. \tag{20}$$

In order to determine the initial condition to enter again a Type I solution for calculating the next cycle ones need to keep track of time. By defining $w^* = 0$ to be the entrance point for Type I solutions we can calculate the time t^* it would take w_n to reach $w^* = 0$.

$$\frac{w^* - w_n}{\gamma} = -\frac{w_n}{\gamma} = \beta^+ \int_{nT}^{nT+t^*} (mt + c_0)dt + t^*, \tag{21}$$

Rearranging (21), we find $t^* = \frac{-b+\sqrt{(b-2m(1+\delta)\frac{w_n}{\gamma})}}{(1+\delta)m}$ and the initial conditions are given in the form of $(s^*,0)$ where $s^* = m(nT+t^*)+c_0$.

Putting all this together, we have arrived at a method that allows us in principal to deduce a first return map of the chaotic SIR equations. In so doing we have arrived at an explicit expression for the number of fadeouts that can be expected, and the conditions which control this number. Thus for the first time fadeouts can be understood and predicted in terms of explicit epidemiological parameters. Finally, we are able to see more directly the mechanism of synchronization through unidirectional coupling or one-way driving, and we are planning to explore this in much more detail with this framework.

CONCLUDING REMARKS

Over the last ten years physicists have invested a great deal of effort in studying the theory of synchronization. Most of this effort has been directed towards understanding chaotic synchronization of model systems. Much less is known about synchronization phenomena in natural systems [7, 13]. In this paper we investigated four different forms of complex biological synchronization using a range of different theoretical approaches, in an attempt to cross the bridge between the fields of physics and ecology. We believe that with the help of tools from nonlinear dynamics, these examples should provide inspiration and motivation for furthering our understanding of the diverse but subtle aspects of synchronization.

ACKNOWLEDGMENTS

L.S., A.H. and R.O. were supported by the McDonnell Foundation and EU grant Phytoplankton On-Line; B.B. was supported by the German Volkswagen-Stiftung.

REFERENCES

1. Maynard-Smith, J., *Anim. Behav.*, **25**, 1–9 (1977).
2. Myers, J. H., *Advances in Ecol. Research*, **18**, 179–242 (1988).
3. Kaneko, K., *Physica D*, **41**, 137–149 (1990).
4. Earn, D. J. D., Rohani, P., Bolker, B. M., and Grenfell, B., *Science*, **287**, 667–670 (2000).
5. Earn, D. J. D., Levin, S. A., and Rohani, P., *Science*, **290**, 1360–1363 (2000).
6. Cazelles, B., *Phys Rev. E*, in press.
7. Blasius, B., Huppert, A., and Stone, L., *Nature*, **399**, 354–359 (1999).
8. Blasius, B., and Stone, L., *Int. J. Bif. and Chaos*, **10**, 2361–2380 (2000).
9. Cazelles, B., and Boudjema, G., *Am. Nat.*, **157**, 670–676 (2001).
10. Vandermeer, J., Stone, L., and Blasius, B., *Chaos, Solitons and Fractals*, **12**, 265–276 (2001).
11. Huppert, A., Blasius, B., and Stone, L., *American Naturalist*, in press.
12. Schwartz, I. B., and Erneux, T., *SIAM J. Appl. Math.*, **54**, 1083–1100 (1994).
13. Blasius, B., and Stone, L., *Nature*, **406**, 846–847 (2000).